

COOD: Concept-based Zero-shot OOD Detection

Zhendong Liu^{1,*} Yi Nian^{2,*} Henry Peng Zou³ Li Li¹ Xiyang Hu⁴ Yue Zhao¹
¹University of Southern California ²University of Chicago ³University of Illinois Chicago
⁴Carnegie Mellon University

lzd233a@gmail.com, nian@uchicago.edu, pzou3@uic.edu,
{li.li02, yzhao010}@usc.edu, xiyanghu@cmu.edu

*Co-first authors

Abstract

How can models effectively detect out-of-distribution (OOD) samples in complex, multi-label settings without extensive retraining? Existing OOD detection methods struggle to capture the intricate semantic relationships and label co-occurrences inherent in multi-label settings, often requiring large amounts of training data and failing to generalize to unseen label combinations. While large language models have revolutionized zero-shot OOD detection, they primarily focus on single-label scenarios, leaving a critical gap in handling real-world tasks where samples can be associated with multiple interdependent labels. To address these challenges, we introduce COOD, a novel zero-shot multi-label OOD detection framework. COOD leverages pre-trained vision-language models, enhancing them with a concept-based label expansion strategy and a new scoring function. By enriching the semantic space with both positive and negative concepts for each label, our approach models complex label dependencies, precisely differentiating OOD samples without the need for additional training. Extensive experiments demonstrate that our method significantly outperforms existing approaches, achieving approximately 95% average AUROC on both VOC and COCO datasets, while maintaining robust performance across varying numbers of labels and different types of OOD samples.

1. Introduction

As machine learning (ML) models become essential in a range of real-world applications, out-of-distribution (OOD) detection has gained increasing importance [36]. OOD detection is particularly critical in fields such as autonomous driving [3], medical diagnostics [10], and surveillance [29], where managing data that deviates from the training distribution—known as in-distribution (ID)—is necessary to avoid safety risks or incorrect decisions [9]. Thus, developing robust OOD detection techniques is key to ensuring model reliability in unpredictable environments.

Large Models for OOD Detection (LM-OOD). The rise of large models, particularly Vision-Language Models (VLMs) and MultiModal Large Language Models (MLLMs), has redefined the landscape of OOD detection [34]. Traditional OOD methods, such as Maximum Softmax Probability (MSP) and Mahalanobis distance-based techniques [15], typically require extensive task-specific training on in-distribution (ID) data. In contrast, LLM-based methods leverage pre-trained knowledge, allowing for *zero-shot* and *few-shot* OOD detection capabilities. Models like CLIP [27] exemplify this shift by achieving effective OOD detection with minimal task-specific training, relying on robust, pre-trained representations from multimodal datasets. Recent advancements, such as NegLabel [11], refine zero-shot OOD detection by introducing negative mining strategies to identify semantically meaningful OOD categories. This approach highlights that carefully selected negative labels can significantly improve detection performance without retraining. LM-OOD methods offer distinct advantages over traditional approaches, including strong performance in limited data, high adaptability across various tasks, and improved computational efficiency through reduced dependence on task-specific data preparation and retraining [22, 24, 34].

Limitations in Current LM-OOD. Large models for OOD detection are primarily designed for single-label tasks, where each input corresponds to a single, definitive label [6, 22]. However, many real-world applications are inherently multi-label in nature: medical imaging often requires identifying multiple coexisting conditions [10, 12]. Current state-of-the-art methods like NegLabel [11] encounter limitations in these multi-label contexts, as seen in Fig. 1: First, the complexity of semantic similarity computations increases significantly with multiple concurrent labels compared to single labels. Second, these methods assume OOD samples are semantically distant from ID classes, which may not hold in multi-label settings where novel combinations of known concepts could form valid OOD cases [25, 33]. Additionally, these approaches struggle to effectively model complex label

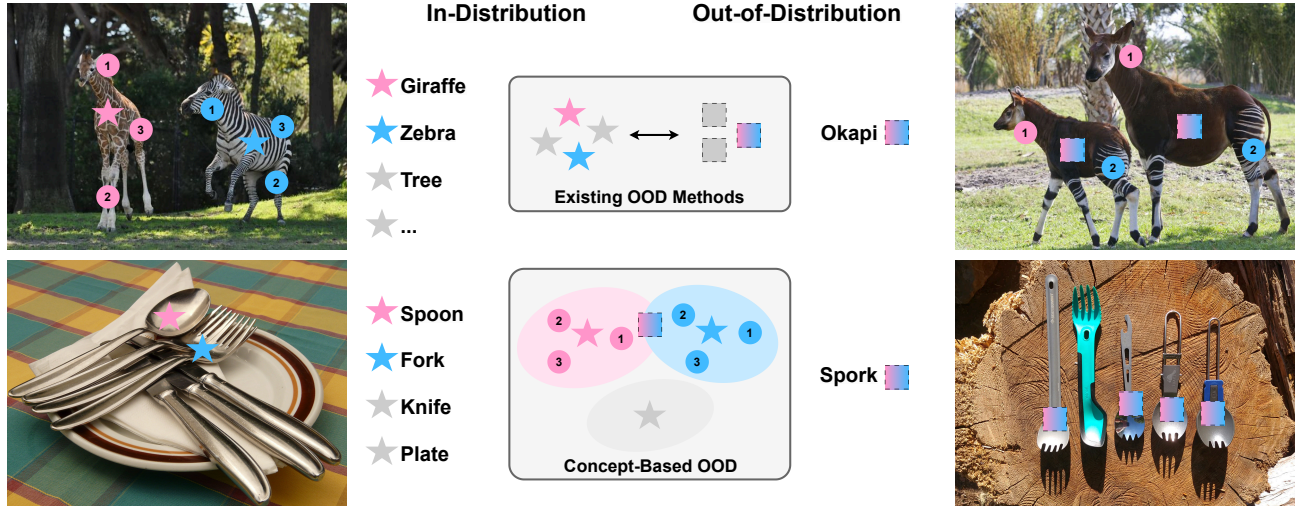


Figure 1. Motivation for Concept-Based OOD Detection. Traditional methods struggle with complex multi-label cases. Our approach expands the label space with positive and negative concepts, enabling robust detection of complex OOD samples like “Okapi” and “Spork.”

co-occurrence patterns and conditional dependencies, both crucial in multi-label contexts [37, 39]. These limitations highlight an essential gap in adapting LM-OOD methods for multi-label tasks, where it is necessary to differentiate between known and unknown label combinations within complex label spaces for practical application [24, 36].

Our Proposal: Extending LM-OOD to Multi-Label Settings. In this work, we introduce COOD (concept-based OOD detection), the first multi-label OOD detection framework that leverages VLM models, specifically CLIP [33], in a zero-shot setting. COOD addresses the challenges of multi-label OOD detection by incorporating a concept-based label expansion strategy. It enriches the base label set with two fine-grained concepts: positive concepts, which capture complex semantic details closely related to ID classes, and negative concepts, which, filtered by a similarity threshold, introduce semantically distant features to strengthen ID-OOD separation. COOD embeds these expanded concept labels alongside the original base labels, creating a refined semantic space that enables precise detection of subtle differences between ID and OOD samples, without additional training. By leveraging CLIP’s extensive pre-trained multi-modal knowledge, COOD achieves robust and flexible OOD detection in complex, multi-label scenarios.

Our technical contributions are summarized as follows:

- **Novel Multi-label OOD Detection:** We present a novel multi-label OOD detection framework based on the CLIP to achieve zero-shot detection without additional training.
- **Concept-based Label Expansion:** We introduce a concept-based label expansion that leverages positive and negative concepts for precise discrimination of OOD samples and provide interpretability in multi-label tasks.
- **Effectiveness:** Our method demonstrates superior performance across standard benchmarks, outperforming exist-

ing methods in multi-label OOD detection while maintaining efficiency and robustness in real-world settings. Our method achieves an OOD sample detection efficiency of approximately 800 images per second on the CLIP-B/16.

2. Proposed COOD Method

2.1. Preliminaries on OOD Detection

In multi-label OOD detection, we aim to determine whether a given input image $I \in \mathcal{I}$ belongs to the ID or represents an unknown OOD sample. We denote the set of base labels as $\mathcal{B} = \{\ell_1, \ell_2, \dots, \ell_{|\mathcal{B}|}\}$, representing known classes within the ID. Each image I can be associated with multiple labels from \mathcal{B} , capturing the multi-label nature of this task.

To formalize this, we define a scoring function, $S_{ID} : \mathcal{I} \rightarrow \mathbb{R}$, which assigns an ID score to each image. For simplicity, we frame our approach around this ID score rather than the OOD score, with the following criteria:

$$S_{ID}(I) \begin{cases} > \gamma, & \text{if } I \sim \mathcal{D}_{ID}, \\ \leq \gamma, & \text{if } I \sim \mathcal{D}_{OOD}, \end{cases} \quad (1)$$

where γ is a threshold determined through validation, and \mathcal{D}_{ID} and \mathcal{D}_{OOD} are ID and OOD distributions, respectively. In this setup, S_{ID} provides a measure of similarity to the ID distribution, aiding in distinguishing between known and unknown samples in a multi-label context.

2.1.1. Revisit VLM-based OOD Detection

Vision-Language Models (VLMs) bring powerful multi-modal capabilities for OOD detection, allowing more flexible, context-aware identification of OOD samples [24, 34]. Large-scale pre-trained VLMs, such as CLIP [27] and GPT-4V [38], enable models to process images and text prompts together, enhancing adaptability and precision across diverse visual and textual domains [6].

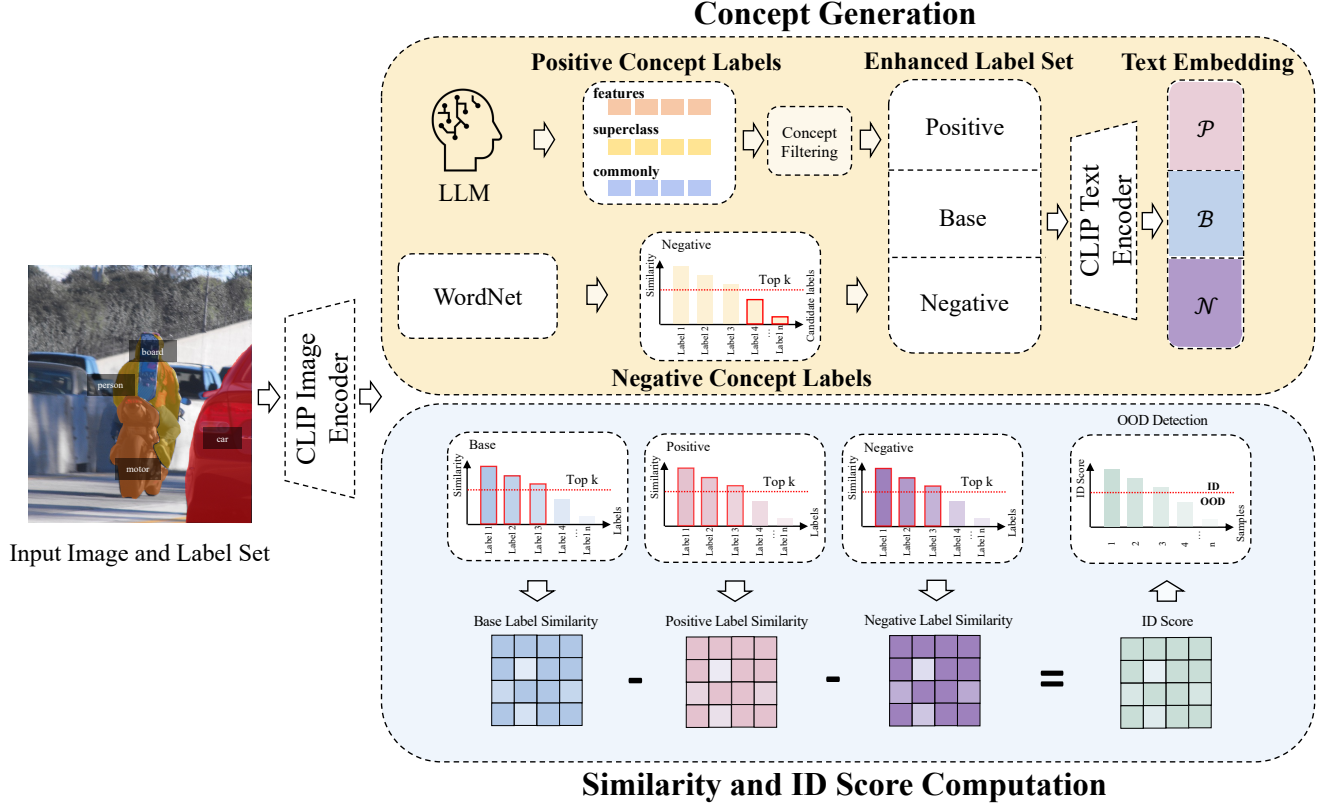


Figure 2. Overview of COOD (§2.2). The Concept Generation module (§2.3) uses LLMs to expand base labels into positive (\mathcal{P}) and negative (\mathcal{N}) concept sets, enhancing the ID-OOD boundary. Positive concepts capture fine-grained, ID-aligned features, while negative concepts provide contrasting OOD-aligned features. The Similarity and ID Score Computation module (§2.4) encodes an input image and computes similarity scores with \mathcal{P} , \mathcal{B} (base), and \mathcal{N} sets. An ID score based on top- k similarities then classifies the image for ID/OOD.

VLM-based OOD detection generally follows two primary approaches [34]: *Prompting-based Detection*, which directly prompts VLMs to respond with OOD indicators [1], and *Contrasting-based Detection*, which uses multimodal VLMs pre-trained with contrastive objectives to distinguish OOD samples [22]. This work focuses on the contrasting-based approach in multimodal contexts, as it is well-suited for enhancing OOD detection by amplifying distinctions between ID and OOD classes. Methods like NegLabel [11] and NegPrompt [16] fall under this category. NegLabel enhances OOD detection by introducing negative labels to contrast with in-distribution (ID) classes, while NegPrompt uses learned negative prompts to emphasize OOD differences by contrasting them with ID prompts. **Formal Definition.** The OOD detection score $S(x)$ for a sample x is defined as:

$$S_{OOD}(x) = \frac{\sum_{i \in Y} \exp(\text{sim}(h, e_i))}{\sum_{i \in Y} \exp(\text{sim}(h, e_i)) + \sum_{j \in Y^-} \exp(\text{sim}(h, e_j^-))}, \quad (2)$$

where h is the embedding of x ; e_i and e_j^- are embeddings for ID and negative representations (NegPrompt [16] or NegLabel [11]) from sets Y and Y^- , respectively; and

$\text{sim}(h, e)$ denotes the similarity (e.g., cosine similarity) between embeddings. The numerator measures similarity to ID representations, while the denominator incorporates both ID and negative similarities, amplifying the detection signal. Note that, our definition is a little different, a smaller $S(x)$ means a larger probability of x being an OOD sample.

Limitations in Current Approaches. Current methods like NegLabel and NegPrompt assume that OOD classes are semantically distant from ID classes, which may not hold in real-world scenarios. OOD samples can closely resemble ID classes, particularly in fine-grained distinctions (e.g., similar dog breeds), limiting the effectiveness of a purely semantic distance-based approach.

Moreover, extending single-label OOD detection methods [20, 30] to multi-label contexts presents additional challenges. Multi-label settings often involve significant semantic overlap between labels and co-occurring ID and OOD labels, complicating the extraction of effective negative labels or prompts. These issues highlight the need for advanced detection techniques to capture the complex dependencies and relationships inherent in multi-label OOD detection tasks.

2.2. Overview of COOD Method

The COOD framework improves OOD detection by refining the decision boundary between ID and OOD samples using fine-grained concepts. By introducing positive and negative concept sets, \mathcal{P} and \mathcal{N} , COOD leverages LLMs to add contextual information around ID samples, thereby enhancing sensitivity to OOD cases.

COOD is built on two core components (see Fig. 2):

1. **Concept Generation and Similarity Measure (§2.3):** To distinguish ID from OOD samples, we generate positive concepts (\mathcal{P}) and negative concepts (\mathcal{N}) that are closely and distantly related to ID classes, respectively. Positive concepts, mined using LLMs, capture domain-relevant features of ID samples at a fine-grained level, while negative concepts are chosen based on their semantic distance from ID classes to enhance contrast.
2. **Similarity and ID Score Computation (§2.4):** For each input image I , we compute similarity scores with these concept sets and the base label set \mathcal{B} , forming a robust semantic space for evaluating ID-OOD relationships. After this, we define an ID score $S_{\text{ID}}(I)$ that aggregates the image’s alignment with ID concepts (\mathcal{B} and \mathcal{P}) and contrasts it with the negative concepts (\mathcal{N}). When this score falls below a predefined threshold γ , the image is classified as OOD. This scoring method sharpens the decision boundary by leveraging contrasts between positive and negative concepts, giving more accurate OOD detection.

The pseudocode in Algo. 1 outlines the full procedure for COOD. To formalize the OOD detection decision, we compute an ID score and classify an image X as OOD if this score falls below a threshold γ . Specifically, the decision function \tilde{Y} is defined as follows:

$$\tilde{Y} = \mathbb{I}(S_{\text{ID}}(h, P, N) < \gamma), \quad \text{where } h = f_{\text{img}}(X), \quad (3)$$

$$P = f_{\text{text}}(\text{prompt}(\mathcal{P})), \quad N = f_{\text{text}}(\text{prompt}(\mathcal{N})).$$

Here, h is the image embedding for X , obtained using an image encoder f_{img} , while P and N are the positive and negative concept embeddings generated via text prompts for concept sets \mathcal{P} and \mathcal{N} , respectively. The indicator function \mathbb{I} produces the final OOD classification.

Theoretical Justification. we derive theoretical bounds (§2.5) that validate the scoring function’s effectiveness in assigning higher scores to ID samples than OOD samples, underscoring the robustness of our approach.

Advantages. The proposed COOD approach is computationally efficient, leveraging pre-trained embeddings without requiring additional model training. By incorporating positive and negative concepts, the model gains enhanced semantic understanding, allowing for clearer differentiation between ID and OOD samples. The focus on top- k similarity values makes the method robust to noise, ensuring stable performance across varied datasets and label sets.

Algorithm 1 Multi-Label OOD Detection with COOD

Require: Image I , base label set \mathcal{B} , threshold γ , top- k parameter k

Ensure: Classification of I as ID or OOD

- 1: **Concept Generation (§2.3):** Generate positive concepts \mathcal{P} and negative concepts \mathcal{N} using an LLM.
 - 2: **Embedding Computation:** Compute embeddings for I , as well as for each label in \mathcal{B} , \mathcal{P} , and \mathcal{N} .
 - 3: **Top- k Similarity Calculation (§2.4):** Calculate the top- k mean similarity scores, $\mu_k(\mathcal{B}, I)$, $\mu_k(\mathcal{P}, I)$, and $\mu_k(\mathcal{N}, I)$.
 - 4: **ID Score Computation (§2.4):** Using the top- k similarities, compute the ID score $S_{\text{ID}}(I)$ according to Eq. (7).
 - 5: **Decision:** if $S_{\text{ID}}(I) > \gamma$ then classify I as ID; else classify I as OOD.
-

2.3. Concept Generation

Motivation. The concept generation process in COOD creates a rich semantic space to strengthen ID-OOD distinctions. By constructing a set of positive concepts, \mathcal{P} , closely aligned with ID samples, and a set of negative concepts, \mathcal{N} , that enhances the contrast with OOD samples, we can refine the decision boundary between ID and OOD.

Positive Concept Mining \mathcal{P} . To build a comprehensive set of positive concepts that accurately represents ID characteristics, we use a two-stage approach inspired by LF-CBM [26]. This process enriches each base label by capturing specific attributes that reinforce its identity within the ID class.

1. **Concept Querying:** We prompt GPT-4 to generate concepts in three distinct contexts for each target object, using structured prompts tailored to elicit three categories: features (prompt $_F$), superclasses (prompt $_S$), and commonly associated items (prompt $_C$). This contextual querying ensures that each concept captures detailed, complex information, improving the clarity and consistency of the concept pool. Each prompt is crafted to encourage concise, relevant responses without qualifiers, which enhances precision, detailed in the Appendix ??.
2. **Concept Filtering:** After generating these candidate concepts, we apply filtering criteria to retain only the most distinctive and relevant features. This step is essential to ensure that the concept set effectively captures the ID characteristics required to differentiate ID from OOD. Our filtering process, detailed in the Appendix ??, refines the generated concepts into a cohesive and meaningful set of positive labels.

The final positive concept set, \mathcal{P} , is constructed as:

$$\mathcal{P} = \bigcup_{c_i \in \mathcal{B}} (\text{prompt}_F(c_i) \cup \text{prompt}_S(c_i) \cup \text{prompt}_C(c_i)), \quad (4)$$

where \mathcal{B} denotes the set of ID labels, and each $c_i \in \mathcal{B}$ is queried to generate its positive concept labels.

Negative Concept Mining \mathcal{N} . To reinforce the distinction between ID and OOD samples, we develop a set of negative concepts, \mathcal{N} , using a process called NegMining [11]. This approach helps us identify concepts that are semantically distant from ID labels, forming a contrasting boundary that enhances OOD detection.

Starting with a large collection of words from a lexical database like WordNet, we create a candidate label space $\mathcal{N}^c = \{n_1, n_2, \dots, n_C\}$. For each candidate label \tilde{n}_i in this set, we calculate a similarity score based on its cosine similarity with the entire ID label set, ensuring that the chosen negative concepts have minimal alignment with ID labels.

- For each ID label $l \in \mathcal{B}$, we obtain its text embedding e_l using a text encoder f^{text} .
- For each candidate $\tilde{n}_i \in \mathcal{N}^c$, we compute its embedding:

$$\tilde{e}_i = f^{\text{text}}(\text{prompt}(\tilde{n}_i)). \quad (5)$$

We select the top candidates with the smallest similarity scores relative to the ID label set, forming a set of negative labels that are maximally distant from ID concepts.

The final negative concept set is defined as:

$$\begin{aligned} \mathcal{N} &= \{n \mid \text{Sim}(\tilde{n}_i, \mathcal{B}) < \tau_i\}, \\ \tau_i &= \text{percentile}_\eta(\{\text{Sim}(\tilde{e}_i, e_l)\}_{l \in \mathcal{B}}), \end{aligned} \quad (6)$$

where $\text{Sim}(\tilde{n}_i, \mathcal{B})$ represents the similarity between candidate \tilde{n}_i and the ID set \mathcal{B} , and τ_i is the η -th percentile of similarity scores, providing robustness against outliers.

By expanding the base label set \mathcal{B} to include positive concepts \mathcal{P} and contrasting them with negative concepts \mathcal{N} , we create an enriched semantic space. This structure allows for more precise discrimination between ID and OOD samples, capturing both the core characteristics of the ID classes and their semantic boundaries effectively.

2.4. Similarity and ID Score Computation

After generating our positive and negative concepts, COOD computes an ID score for each input image I , based on its similarity with the positive concept set \mathcal{P} , negative concept set \mathcal{N} , and base labels \mathcal{B} . This score helps determine if the image aligns more closely with ID or OOD characteristics. **ID Score Definition.** The ID score $S_{\text{ID}}(I)$ for an image I is:

$$S_{\text{ID}}(I) = w_{\mathcal{B}} \cdot \mu_k(\mathcal{B}, I) - w_{\mathcal{P}} \cdot \mu_k(\mathcal{P}, I) - w_{\mathcal{N}} \cdot \mu_k(\mathcal{N}, I) \quad (7)$$

where $w_{\mathcal{B}}$, $w_{\mathcal{P}}$, and $w_{\mathcal{N}}$ are weighting coefficients that determine the relative contribution of each set in computing the ID score, reflecting the importance of the base labels \mathcal{B} , positive concepts \mathcal{P} , and negative concepts \mathcal{N} .

Top- k Mean Similarity Calculation. The term $\mu_k(\mathcal{S}, I)$ in Eq. (7) represents the top- k mean similarity score between

the image I and the label set \mathcal{S} , calculated as:

$$\mu_k(\mathcal{S}, I) = \frac{1}{k} \sum_{i=1}^k \text{sim}(h, e_i) \quad (8)$$

where h is the embedding of image I , and e_i are the embeddings of the top- k closest elements in set \mathcal{S} . Here, \mathcal{S} can be any of \mathcal{B} (base labels), \mathcal{P} (positive concepts), or \mathcal{N} (negative concepts). The similarity function $\text{sim}(h, e_i)$ (e.g., cosine similarity) captures the alignment between the image embedding h and each of the concept embeddings e_i .

This top- k similarity measure emphasizes the most relevant matches between the image and the concepts in each set, minimizing the influence of less relevant or noisy features and enhancing robustness in scoring.

Interpretation of the ID Score. The scoring function $S_{\text{ID}}(I)$ captures the degree of alignment of an image with ID or OOD characteristics. For ID samples, we anticipate high alignment with both the base labels \mathcal{B} and positive concepts \mathcal{P} , yielding a high $S_{\text{ID}}(I)$. Conversely, OOD samples will likely align more closely with negative concepts \mathcal{N} , resulting in a lower ID score. By focusing on the top- k similarities, this approach enhances robustness to noise and emphasizes the most semantically relevant features.

This mechanism refines the boundary between ID and OOD samples by leveraging positive and negative contrasts, resulting in more accurate and reliable OOD detection.

2.5. Theoretical Justification

Lemma 1 (Separability of ID-OOD). *The scoring function can distinguish between in-distribution (ID) and out-of-distribution (OOD) samples based on their semantic relationships by appropriately selecting weights $w_{\mathcal{P}}$ and $w_{\mathcal{N}}$.*

Proof. We assume the following bounds on the similarity scores $\mu_k(\cdot, \cdot)$ between an image I and class representations in different contexts when I is either ID or OOD:

$$0 \leq \mu_k(\mathcal{B}, I_{\text{OOD}}) \leq a < \mu_k(\mathcal{B}, I_{\text{ID}}) \leq A \leq 1,$$

$$0 \leq \mu_k(\mathcal{P}, I_{\text{OOD}}) \leq b < \mu_k(\mathcal{P}, I_{\text{ID}}) \leq B \leq 1,$$

$$0 \leq \mu_k(\mathcal{N}, I_{\text{ID}}) \leq c < \mu_k(\mathcal{N}, I_{\text{OOD}}) \leq C \leq 1.$$

To establish separability between ID and OOD samples, we examine bounds on the scoring function for in-distribution and out-of-distribution images.

1. **Lower Bound for S_{ID} :** Based on the assumed bounds, the lower bound of the scoring function S_{ID} for ID samples is: $S_{\text{ID}}^{\text{lower}} = w_{\mathcal{B}}a - w_{\mathcal{P}}B - w_{\mathcal{N}}c$.

2. **Upper Bound for S_{ID} :** The upper bound of the scoring function S_{ID} for OOD samples is: $S_{\text{ID}}^{\text{upper}} = w_{\mathcal{B}}a - w_{\mathcal{N}}C$.

3. **Separability Condition:** For the scoring function to effectively distinguish between ID and OOD samples, we

require: $S_{ID}^{lower} - S_{ID}^{upper} > 0$. Substituting the expressions for S_{ID}^{lower} and S_{ID}^{upper} , this simplifies to: $w_P B < w_N (C - c)$.

By selecting w_P and w_N to satisfy this condition, we ensure that the scoring function S_{ID} can differentiate between ID and OOD samples based on semantic similarity. \square

Implications. This lemma establishes a theoretical basis for using the scoring function to distinguish ID from OOD samples by focusing on top- k similarities, enhancing robustness by minimizing the effect of weakly relevant labels.

3. Experimental Results

3.1. Experimental Setup

Datasets and Settings. We evaluate our proposed multi-label OOD detection method on widely used datasets. For ID datasets, we use Pascal VOC [5], MS-COCO [19], and Objects365 [28]. For OOD datasets, we use Textures [2] and Filtered ImageNet22K [8]. These datasets provide diverse categories and rich multi-label annotations, making them ideal for assessing OOD detection in complex real-world scenarios. To quantify the OOD detection performance, we report two standard metrics, **FPR@95** and **AUROC**. See Appx. ?? for more datasets and metrics details.

Implementation Details. Our method is implemented using PyTorch and evaluated on NVIDIA 3090 GPU. As a zero-shot approach, our method leverages pre-computed concept embeddings and does not require any additional training. This results in a computationally efficient solution, with an average inference time of approximately 800 images per second. This efficient design allows for parallelized OOD detection alongside zero-shot classification tasks, making it suitable for deployment in real-time applications. For reproducibility, all hyperparameters and settings follow standard configurations, and further implementation details are provided in Appx. ??.

3.2. Experimental Results and Analysis

OOD Detection Performance Comparison. Table 1 presents a comparison of the OOD detection performance of COOD against several baseline approaches. Where * represents our reproduction of the missing results from the original paper, and † means that we used the values from the original paper, and †* represents the best value we take from the replicated results and the reported results in the original paper. The gray boxes represent our approach. In addition, **(Joint)-Energy** denotes the better of the JointEnergy [32] method and the Energy [20] method. **Bold** values indicate the best results. *Our method demonstrates strong OOD detection performance across both ResNet-based and ViT-based architectures.* Specifically, our ResNet-based CLIP achieves superior results, particularly on the Pascal VOC ID dataset and Textures OOD dataset, with FPR95 of 8.76% and AUROC of 97.79%, outperforming all baseline methods.

These suggest that the ResNet-based architecture may be particularly effective in handling texture-oriented datasets.

On the ViT-based CLIP, our method achieves the lowest FPR95 of 23.87% on the Pascal VOC dataset and outperforms competing methods on the COCO dataset, achieving an impressive AUROC of 95.07%. The ViT-based approach performs exceptionally well across most datasets, indicating that the ViT architecture enhances OOD detection across diverse image distributions, while still maintaining strong robustness on texture-based datasets.

Importantly, our approach operates as a *zero-shot* method, requiring no additional training or complex parameter tuning. This makes it highly efficient with low computational overhead. This contrasts with other multi-label classifiers requires training. For method without training, such as SeTAR [17], which requires extensive parameter search time, impacting practical deployment. Overall, our method provides an efficient and effective zero-shot solution for OOD detection, yielding state-of-the-art performance with minimal overhead on both architectures.

3.3. Visual Interpretability of COOD Components

Figure 3 presents a detailed interpretability analysis of COOD through a t-SNE visualization [31] of text embeddings and several qualitative examples. The interpretability of COOD is a key feature, as it allows us to visualize and understand how specific concepts contribute to OOD detection. **t-SNE Visualization.** The t-SNE plot on the left side of Fig. 3 visualizes the embeddings of concepts from our model, showing a clear separation between ID labels (Pascal VOC, shown in red) and OOD concepts. Notably, the embeddings for positive concepts (shown in red) form distinct clusters separate from negative concepts (shown in blue). This clustering reflects the model’s ability to encode meaningful semantic information that distinguishes ID from OOD samples. The clustering of positive concepts around ID points and the scattering of negative concepts in more distant regions confirm that the model effectively captures relationships that contribute to its decision-making process.

Qualitative Examples. The right side of Fig. 4 provides several example images with corresponding bar plots, illustrating the concept weights associated with each image. In each bar plot, positive concepts are marked in red, while negative concepts are marked in blue. This visual representation offers insight into which semantic features are influencing the OOD score, making it easier to interpret why certain samples are classified as ID or OOD.

3.4. Ablation Studies and Additional Analysis

To assess the contributions of different components in our approach, we conduct an ablation study with variations in the parameters $top-k$, S_A , and S_B on the Pascal VOC and COCO datasets, as shown in Table 2. For more experiments on different model architectures and OOD score functions,

Table 1. OOD Detection Results on Various Datasets. Our ViT-based CLIP model achieves strong performance with the lowest FPR95 and highest AUROC across most datasets, outperforming standard OOD methods. The ResNet-based CLIP variant also performs competitively.

| ID Dataset OOD Dataset Method | Pascal VOC | | | | COCO | | | | ImageNet | |
|--|--------------|--------------|-------------|--------------|--------------|--------------|--------------|--------------|--------------|--------------|
| | ImageNet22k | | Textures | | ImageNet22k | | Textures | | Textures | |
| | FPR95↓ | AUROC↑ | FPR95↓ | AUROC↑ | FPR95↓ | AUROC↑ | FPR95↓ | AUROC↑ | FPR95↓ | AUROC↑ |
| ResNet-based Multi-label Classifier | | | | | | | | | | |
| MaxLogit* [8] | 36.32 | 91.04 | 12.36 | 96.22 | 44.47 | 87.13 | 19.83 | 95.31 | 57.09 | 86.71 |
| MSP* [7] | 69.85 | 78.24 | 41.81 | 89.76 | 82.15 | 67.47 | 65.21 | 81.88 | 68.00 | 79.61 |
| ODIN* [18] | 36.32 | 91.04 | 12.36 | 96.22 | 54.51 | 84.92 | 33.15 | 90.71 | 50.23 | 85.62 |
| (Joint)-Energy* [20, 32] | 31.96 | 92.32 | 10.87 | 96.78 | 41.81 | 90.30 | 17.72 | 96.07 | 53.72 | 85.99 |
| Ours (ResNet-based CLIP) | 25.28 | 93.32 | 8.76 | 97.79 | 26.83 | 93.14 | 10.53 | 97.17 | 43.72 | 91.68 |
| ViT-based CLIP | | | | | | | | | | |
| MSP† [7] | 86.35 | 75.42 | 64.74 | 85.46 | 59.27 | 87.30 | 45.57 | 90.35 | 64.96 | 78.16 |
| (Joint)-Energy† [20, 32] | 81.93 | 76.59 | 90.18 | 78.23 | 65.39 | 85.20 | 76.01 | 82.40 | 51.18 | 88.09 |
| MCM†* [22] | 73.81 | 80.37 | 53.67 | 88.52 | 63.34 | 86.10 | 49.22 | 89.11 | 57.77 | 86.11 |
| GL-MCM†* [24] | 72.98 | 81.76 | 64.74 | 86.96 | 48.96 | 88.50 | 45.06 | 89.70 | 57.41 | 83.73 |
| NegLabel*[11] | 35.83 | 91.18 | 43.14 | 89.72 | 33.24 | 90.19 | 47.33 | 85.10 | 43.56 | 90.22 |
| MCM+SeTAR†* [17] | 48.25 | 92.08 | 40.44 | 93.58 | 73.55 | 80.43 | 47.33 | 89.58 | 55.83 | 86.58 |
| GL-MCM+SeTAR†* [17, 24] | 31.47 | 94.31 | 20.35 | 96.36 | 65.30 | 81.38 | 42.05 | 89.81 | 54.17 | 84.59 |
| Ours (ViT-based CLIP) | 23.87 | 94.32 | 21.58 | 95.14 | 20.37 | 95.07 | 21.63 | 94.53 | 39.41 | 91.10 |

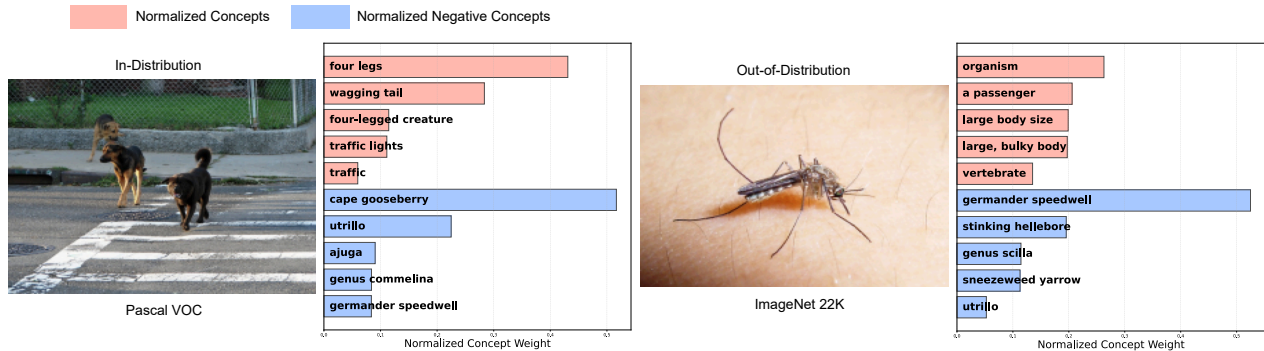


Figure 3. Interpretability analysis of COOD on ID (left) and OOD (right) examples. For ID sample (dogs), positive concepts (e.g., “four-legged creature”) receive high weights, confirming ID alignment. For OOD samples (mosquito), negative concepts dominate.

Table 2. Ablations on Pascal VOC and COCO datasets. Lower *top-k* values (e.g., 0.1, 0.2) improve performance by focusing on key concepts. Using both S_A and S_B together yields the best results, with an FPR95 of 24.78% and AUROC of 94.27% on Pascal VOC.

| Top- <i>k</i> | S_A | S_B | Pascal VOC ID | | COCO ID | |
|---------------|-------|-------|---------------|-------|---------|-------|
| | | | FPR95 | AUROC | FPR95 | AUROC |
| 0.05 | ✗ | ✓ | 39.39 | 89.08 | 26.65 | 94.40 |
| 0.2 | ✗ | ✓ | 36.12 | 91.72 | 48.87 | 89.49 |
| 0.05 | ✓ | ✗ | 45.79 | 90.13 | 28.88 | 92.39 |
| 0.2 | ✓ | ✗ | 36.43 | 91.73 | 33.70 | 90.09 |
| 0.05 | ✓ | ✓ | 36.28 | 91.28 | 20.37 | 95.07 |
| 0.1 | ✓ | ✓ | 28.07 | 93.60 | 24.16 | 93.91 |
| 0.2 | ✓ | ✓ | 24.78 | 94.27 | 29.08 | 92.39 |
| 0.3 | ✓ | ✓ | 26.76 | 93.62 | 32.95 | 91.02 |
| 0.5 | ✓ | ✓ | 32.23 | 91.82 | 39.61 | 88.48 |

please refer to the Appendix ???. Recall that we defined the score function in Eq. (7). Here, we simplify the score

Table 3. Representative OOD Detection Performance on Pascal VOC (Textures) with Different Architectures and Distance Metrics

| Architecture | Distance Metric | FPR95 | AUROC |
|--------------|-------------------|-------|-------|
| ResNet50 | mean | 8.76 | 97.79 |
| ResNet50x16 | mean | 18.54 | 95.89 |
| ViT-B/16 | mean | 21.58 | 95.14 |
| ViT-B/16 | percentile (0.75) | 26.62 | 93.99 |
| ViT-L/14 | mean | 24.28 | 94.55 |

function by letting w_B to 2, and w_P and w_N to 1 and let **Score Components** (S_A and S_B) correspond to the two terms in the simplified scoring function:

$$S_{\text{OOD}}(I) = \underbrace{[\mu_k(\mathcal{B}, I) - \mu_k(\mathcal{P}, I)]}_{S_A} + \underbrace{[\mu_k(\mathcal{B}, I) - \mu_k(\mathcal{N}, I)]}_{S_B} \quad (9)$$

Effect of Top-k Selection. The *top-k* parameter controls the number of concepts used in similarity calculations, allowing us to focus on the most relevant information. Lower values of *top-k* (e.g., 0.1 and 0.2) generally yield better results, as they prioritize the top-matching concepts, minimizing noise

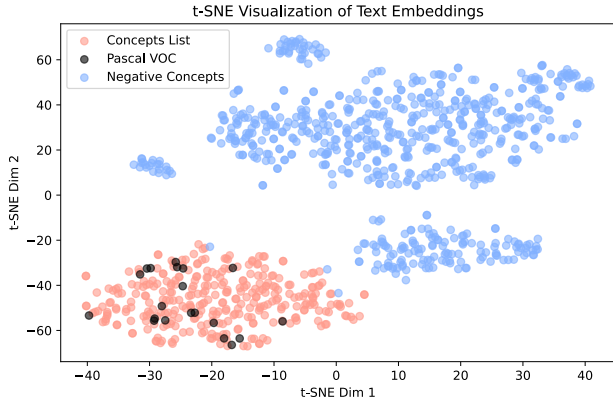


Figure 4. t-SNE plot for text embeddings. This clustering reflects the model’s ability to encode meaningful semantic information that distinguishes ID labels, concepts and negative labels.

from less related features. For instance, with $top-k$ set to 0.1, our approach achieves an FPR95 of 28.07% and an AUROC of 93.6% on Pascal VOC, outperforming larger $top-k$ values which include more potentially distracting concepts.

Impact of S_A and S_B . Enabling both S_A and S_B yields the best performance across metrics. For example, on Pascal VOC, activating both scores reduces FPR95 from 36.12% to 24.78% and boosts AUROC from 91.72% to 94.27%. This improvement indicates that S_A and S_B capture complementary aspects of the data, thereby enhancing the model’s ability to differentiate between ID and OOD samples effectively.

4. Related Work

4.1. Zero-Shot and Multi-Label OOD Detection

With the rise of contrastive learning-based cross-modal models like CLIP, traditional OOD detection methods face new challenges, particularly in zero-shot settings. In addition, the increasing complexity of image understanding tasks has introduced challenges in multi-label OOD detection.

For OOD detection in CLIP-based settings, several methods have been proposed, including both zero-shot and fine-tuning approaches. For example, ZOC [4] introduces a trainable generator and additional data to create extra OOD labels. Maximum Concept Matching (MCM) [22] uses textual embeddings of ID classes as concept prototypes, calculating an MCM score based on the cosine similarity between image and textual features to identify OOD instances. NegLabel [11] enhances OOD detection by incorporating a large set of negative labels, which are semantically distant from in-distribution (ID) labels, thereby improving the model’s ability to distinguish OOD samples. GL-MCM [23] builds upon CLIP by considering both global and local visual-text alignments in the detection process. SeTAR [17] applies selective low-rank approximation to weight matrices with a greedy search algorithm for optimized OOD detection. NegPrompt [25] introduces transferable negative prompts for OOD detection, where each ID class is paired with learnable negative prompts, improving OOD detection by associating OOD

samples more closely with negative prompts. However, these approaches lack a discussion of multi-label scenarios.

In multi-label tasks, some researchers have explored OOD detection as well. The JointEnergy-based method [32] is one of the first to address OOD detection in multi-label scenarios. A later improvement [21] further refines this approach. Additionally, YoOOD [40] explores OOD detection in multi-label tasks, using an object detection model as the backbone. However, these methods do not explore CLIP-based architectures. Methods utilizing multi-label data with CLIP, such as GL-MCM [23] and SeTAR [17], typically focus on curated datasets and fail to address the challenge of detecting OOD samples when multiple classes co-exist in the same image. In contrast, our work is the first to comprehensively explore how to effectively perform zero-shot OOD detection in multi-label tasks using CLIP models.

4.2. Concept Bottlenecks

Concept bottlenecks have emerged as a promising approach to improve model interpretability and robustness by explicitly modeling the intermediate concepts that influence predictions. Koh et al. [14] proposed using a feature extractor and a concept predictor to generate these "bottleneck" concepts, which are then used in a final predictor to determine class labels. Oikarinen et al. [26] introduced the Label-Free Concept Bottleneck Model (LF-CBM), which generates concepts without requiring manually labeled concept data. Instead, it employs unsupervised methods to automatically identify and extract meaningful concepts from the data. Xu et al. [35] introduced Energy-Based Concept Bottleneck Models (ECBM), which learn positive and negative concept embeddings to capture high-order nonlinear interactions between concepts, enabling richer concept explanations. Probabilistic Concept Bottleneck Models (ProbCBMs) [13] integrate uncertainty estimation with concept predictions. Recently, various other CBM variants have emerged, expanding the versatility of this approach. While these methods have been effective in extracting concepts and describing multiple labels within images, to the best of our knowledge, none have directly applied these concept-based techniques to multi-label and complex OOD detection tasks. Our approach focuses on the novel application of concept bottlenecks specifically for improving OOD detection in such settings.

5. Conclusion, Limitations, and Future Work

This work presents an in-depth exploration of using the CLIP model for efficient zero-shot OOD detection in complex multi-label scenarios. Our concept-based approach demonstrates superior OOD detection performance, achieving over 95% average AUROC on VOC and COCO (as ID datasets) with ImageNet and Texture as OOD datasets. Additionally, we conducted extensive experiments to evaluate the explainability and parameter sensitivity of the method.

Our approach relies on the quality of concept generation and the robustness of embeddings from the CLIP model. Future work could investigate adaptive concept generation methods and alternative embedding models to enhance OOD detection performance in complex multi-label environments.

Broader Impact Statement: COOD enhances multi-label OOD detection, focusing on fine-grained concept differentiation to improve model reliability in applications like healthcare, autonomous systems, and security. By increasing robustness to unknown data, COOD supports safer, more reliable performance in dynamic, high-stakes environments, reducing risks tied to novel or evolving data patterns.

References

- [1] Yunkang Cao, Xiaohao Xu, Chen Sun, Xiaonan Huang, and Weiming Shen. Towards generic anomaly detection and understanding: Large-scale visual-linguistic model (gpt-4v) takes the lead. *arXiv preprint arXiv:2311.02782*, 2023. 3
- [2] M. Cimpoi, S. Maji, I. Kokkinos, S. Mohamed, , and A. Vedaldi. Describing textures in the wild. In *Proceedings of the IEEE Conf. on Computer Vision and Pattern Recognition (CVPR)*, 2014. 6
- [3] Amine Elhafsi, Rohan Sinha, Christopher Agia, Edward Schmerling, Issa AD Nesnas, and Marco Pavone. Semantic anomaly detection with large language models. *Autonomous Robots*, 2023. 1
- [4] Sepideh Esmaeilpour, Bing Liu, Eric Robertson, and Lei Shu. Zero-shot out-of-distribution detection based on the pre-trained model clip. In *Proceedings of the AAAI conference on artificial intelligence*, pages 6568–6576, 2022. 8
- [5] Mark Everingham, Luc Van Gool, Christopher KI Williams, John Winn, and Andrew Zisserman. The pascal visual object classes (voc) challenge. *International journal of computer vision*, 88:303–338, 2010. 6
- [6] Stanislav Fort, Jie Ren, and Balaji Lakshminarayanan. Exploring the limits of out-of-distribution detection. *Advances in Neural Information Processing Systems*, 2021. 1, 2
- [7] Dan Hendrycks and Kevin Gimpel. A baseline for detecting misclassified and out-of-distribution examples in neural networks. *arXiv preprint arXiv:1610.02136*, 2016. 7
- [8] Dan Hendrycks, Steven Basart, Mantas Mazeika, Mohammadreza Mostajabi, Jacob Steinhardt, and Dawn Song. A benchmark for anomaly segmentation. *arXiv preprint arXiv:1911.11132*, 1(2):5, 2019. 6, 7
- [9] Dan Hendrycks, Steven Basart, Mantas Mazeika, Andy Zou, Joe Kwon, Mohammadreza Mostajabi, Jacob Steinhardt, and Dawn Song. Scaling out-of-distribution detection for real-world settings. *arXiv preprint arXiv:1911.11132*, 2019. 1
- [10] Chaoqin Huang, Aofan Jiang, Jinghao Feng, Ya Zhang, Xinchao Wang, and Yanfeng Wang. Adapting visual-language models for generalizable anomaly detection in medical images. 2024. 1
- [11] Xue Jiang, Feng Liu, Zhen Fang, Hong Chen, Tongliang Liu, Feng Zheng, and Bo Han. Negative label guided ood detection with pretrained vision-language models. *arXiv preprint arXiv:2403.20078*, 2024. 1, 3, 5, 7, 8
- [12] Daniel S Kermany, Michael Goldbaum, Wenjia Cai, Carolina CS Valentim, Huiying Liang, Sally L Baxter, Alex McKeown, Ge Yang, Xiaokang Wu, Fangbing Yan, et al. Identifying medical diagnoses and treatable diseases by image-based deep learning. *Cell*, 172(5):1122–1131, 2018. 1
- [13] Eunji Kim, Dahuin Jung, Sangha Park, Siwon Kim, and Sungroh Yoon. Probabilistic concept bottleneck models. *arXiv preprint arXiv:2306.01574*, 2023. 8
- [14] Pang Wei Koh, Thao Nguyen, Yew Siang Tang, Stephen Mussmann, Emma Pierson, Been Kim, and Percy Liang. Concept bottleneck models. In *International conference on machine learning*, pages 5338–5348. PMLR, 2020. 8
- [15] Kimin Lee, Kibok Lee, Honglak Lee, and Jinwoo Shin. A simple unified framework for detecting out-of-distribution samples and adversarial attacks. *Advances in neural information processing systems*, 31, 2018. 1
- [16] Tianqi Li, Guansong Pang, Xiao Bai, Wenjun Miao, and Jin Zheng. Learning transferable negative prompts for out-of-distribution detection. 2024. 3
- [17] Yixia Li, Boya Xiong, Guanhua Chen, and Yun Chen. Setar: Out-of-distribution detection with selective low-rank approximation, 2024. 6, 7, 8
- [18] Shiyu Liang, Yixuan Li, and Rayadurgam Srikant. Enhancing the reliability of out-of-distribution image detection in neural networks. *arXiv preprint arXiv:1706.02690*, 2017. 7
- [19] Tsung-Yi Lin, Michael Maire, Serge Belongie, James Hays, Pietro Perona, Deva Ramanan, Piotr Dollár, and C Lawrence Zitnick. Microsoft coco: Common objects in context. In *Computer Vision—ECCV 2014: 13th European Conference, Zurich, Switzerland, September 6–12, 2014, Proceedings, Part V 13*, pages 740–755. Springer, 2014. 6
- [20] Weitang Liu, Xiaoyun Wang, John Owens, and Yixuan Li. Energy-based out-of-distribution detection. *Advances in Neural Information Processing Systems*, 2020. 3, 6, 7
- [21] Yihan Mei, Xinyu Wang, Dell Zhang, and Xiaoling Wang. Multi-label out-of-distribution detection with spectral normalized joint energy. In *Asia-Pacific Web (APWeb) and Web-Age Information Management (WAIM) Joint International Conference on Web and Big Data*, pages 31–45. Springer, 2024. 8
- [22] Yifei Ming, Ziyang Cai, Jiuxiang Gu, Yiyou Sun, Wei Li, and Yixuan Li. Delving into out-of-distribution detection with vision-language representations. *Advances in Neural Information Processing Systems*, 2022. 1, 3, 7, 8
- [23] Atsuyuki Miyai, Qing Yu, Go Irie, and Kiyoharu Aizawa. Zero-shot in-distribution detection in multi-object settings using vision-language foundation models. *arXiv preprint arXiv:2304.04521*, 2023. 8
- [24] Atsuyuki Miyai, Jingkan Yang, Jingyang Zhang, Yifei Ming, Yueqian Lin, Qing Yu, Go Irie, Shafiq Joty, Yixuan Li, Hai Li, et al. Generalized out-of-distribution detection and beyond in vision language model era: A survey. *arXiv preprint arXiv:2407.21794*, 2024. 1, 2, 7
- [25] Jun Nie, Yonggang Zhang, Zhen Fang, Tongliang Liu, Bo Han, and Xinmei Tian. Out-of-distribution detection with negative prompts. 2024. 1, 8
- [26] Tuomas Oikarinen, Subhro Das, Lam M Nguyen, and Tsui-Wei Weng. Label-free concept bottleneck models. *arXiv preprint arXiv:2304.06129*, 2023. 4, 8
- [27] Alec Radford, Jong Wook Kim, Chris Hallacy, Aditya Ramesh, Gabriel Goh, Sandhini Agarwal, Girish Sastry, Amanda Askell, Pamela Mishkin, Jack Clark, et al. Learning transferable visual models from natural language supervision. *International Conference on Machine Learning*, 2021. 1, 2
- [28] Shuai Shao, Zeming Li, Tianyuan Zhang, Chao Peng, Gang Yu, Xiangyu Zhang, Jing Li, and Jian Sun. Objects365: A large-scale, high-quality dataset for object detection. In *Proceedings of the IEEE/CVF international conference on computer vision*, pages 8430–8439, 2019. 6
- [29] Waqas Sultani, Chen Chen, and Mubarak Shah. Real-world anomaly detection in surveillance videos. In *Proceedings*

- of the *IEEE Conference on Computer Vision and Pattern Recognition*, pages 6479–6488, 2018. 1
- [30] Yiyu Sun, Chuan Guo, and Yixuan Li. React: Out-of-distribution detection with rectified activations. *Advances in Neural Information Processing Systems*, 2021. 3
- [31] Laurens Van der Maaten and Geoffrey Hinton. Visualizing data using t-sne. *Journal of machine learning research*, 9(11), 2008. 6
- [32] Haoran Wang, Weitang Liu, Alex Bocchieri, and Yixuan Li. Can multi-label classification networks know what they don't know? *Advances in Neural Information Processing Systems*, 34:29074–29087, 2021. 6, 7, 8
- [33] Hualiang Wang, Yi Li, Huifeng Yao, and Xiaomeng Li. Clipn for zero-shot ood detection: Teaching clip to say no. In *Proceedings of the IEEE/CVF International Conference on Computer Vision*, pages 17221–17231, 2023. 1, 2
- [34] Ruiyao Xu and Kaize Ding. Large language models for anomaly and out-of-distribution detection: A survey. *arXiv preprint arXiv:2409.01980v2*, 2024. 1, 2, 3
- [35] Xinyue Xu, Yi Qin, Lu Mi, Hao Wang, and Xiaomeng Li. Energy-based concept bottleneck models: unifying prediction, concept intervention, and conditional interpretations. *arXiv preprint arXiv:2401.14142*, 2024. 8
- [36] Jingkang Yang, Kaiyang Zhou, Yixuan Li, and Ziwei Liu. Generalized out-of-distribution detection: A survey. *International Journal of Computer Vision*, 2024. 1, 2
- [37] Hsiang-Fu Yu, Prateek Jain, Purushottam Kar, and Inderjit Dhillon. Large-scale multi-label learning with missing labels. *International Conference on Machine Learning*, pages 593–601, 2014. 2
- [38] Jiangning Zhang, Xuhai Chen, Zhucun Xue, Yabiao Wang, Chengjie Wang, and Yong Liu. Exploring grounding potential of vqa-oriented gpt-4v for zero-shot anomaly detection. *arXiv preprint arXiv:2311.02612*, 2023. 2
- [39] Min-Ling Zhang and Zhi-Hua Zhou. A review on multi-label learning algorithms. *IEEE Transactions on Knowledge and Data Engineering*, 26(8):1819–1837, 2014. 2
- [40] Alon Zolfi, Guy Amit, Amit Baras, Satoru Koda, Ikuya Morikawa, Yuval Elovici, and Asaf Shabtai. Yolood: Utilizing object detection concepts for multi-label out-of-distribution detection. In *Proceedings of the IEEE/CVF Conference on Computer Vision and Pattern Recognition*, pages 5788–5797, 2024. 8